Chapter 12
Experimental Determination of Interlaminar Material Properties of Carbon Fiber Composites

Daniel Hartung and Martin Wiedemann

Abstract Non Crimp Fabric (NCF) provides a low-cost potential and competitive advantages for thick composite structures. In this chapter, a method will be presented to determine the interlaminar failure under combined through-thickness load conditions. Additionally, the in-plane failure behaviour of NCF composite is discussed and analysed. A new test setup, based on the idea of Arcan, determines the material properties. Test results of combined through-thickness loading are presented by in the form of a shear-compression failure curve. The tests are reproducible and reliable. The failure envelope is finally used to verify known failure criteria.

12.1 Introduction

Carbon fiber Non Crimp Fabric (NCF) provides advantages for industrial manufacturing i.e. automated preforming capabilities, efficient infusion technologies and thus reduced processing time. NCF materials are made by stitching together adjacent plies with a thin polyester yarn. The use of NCF composites for thick structures is growing; therefore through-thickness stresses cannot be neglected. Consequently, the failure and stress analysis requires the consideration of the three dimensional stress states. Failure of thick composite material is induced by interlaminar stresses between adjacent plies, which cause delaminations. Generally, the delamination strength in the thickness direction is small

D. Hartung
Institute of Composite Structures and Adaptive Systems, German Aerospace Center (DLR e.V.), Lilienthalplatz 7, 38108, Braunschweig, Germany

M. Wiedemann (✉)
Institute of Composite Structures and Adaptive Systems, German Aerospace Center (DLR e.V.), Lilienthalplatz 7, 38108, Braunschweig, Germany
e-mail: martin.wiedemann@dlr.de

M. Wiedemann and M. Sinapius (eds.), *Adaptive, Tolerant and Efficient Composite Structures*, Research Topics in Aerospace, DOI: 10.1007/978-3-642-29190-6_12,

Table 12.1 Maximum strength of unidirectional single ply (fiber: Tenax UTS 5632 12 K, resin: RTM6)

Fiber strength tension	Fiber strength compression	Intralaminar strength tension	Intralaminar strength compression	Intralaminar strength shear
R^t_{11}	R^c_{11}	R^t_{22}	R^c_{22}	R_{12}
[MPa]	[MPa]	[MPa]	[MPa]	[MPa]
2,208	1,095	43	189	72
±84	±0.1	±1.0	±1.0	±5.2

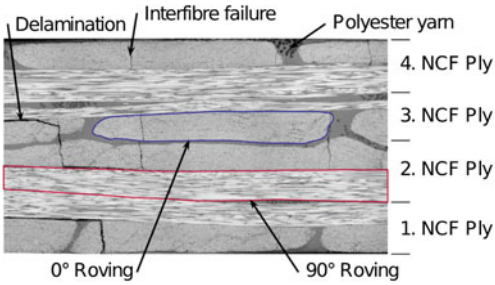

Fig. 12.1 Section of the NCF with characteristic damages

compared to the fiber strength and restricts the applicability of composites structures. To test composite materials in their thickness direction under combined load conditions requires an adequate test device.

12.2 Intra- and Inter-Laminar Failure Behaviour of NCF

It is often assumed that the failure behaviour of fiber composites can be separated into fiber and inter-fiber failure modes: intralaminar (in the laminate plane) and interlaminar (normal to the laminate plane). The allowable material strength along the fiber is significantly higher than the inter-fiber strength. Table 12.1 shows the difference between fiber strength and the intralaminar strength for a carbon Ultra High Tension Strength (UTS) unidirectional single ply.

Due to the multi-axial fiber orientation of NCFs, the failure behaviour of the laminate is in most cases driven by inter-fiber failure modes. Several authors investigated the damage growth of composites under quasi static load conditions. Many of them concluded that micro cracks accumulate continuously during loading and drive the final failure behaviour of composites.

The micrograph image analysis supports this explanation. Figure 12.1 shows different inter-fiber failures, i.e. from micro cracks up to delaminations of a composite that consists of four NCF plies, each with two single plies in an orthogonal orientation. The specimen has been loaded along the 90° direction.

Figure 12.2 shows micrograph images at four strain levels: 0.3, 0.6, 0.75 and 1.5%. No damages can be found at a strain level of 0.3%. At a strain level of 0.6%, first inter-fiber damages in the form of micro cracks inside of a roving can be found.

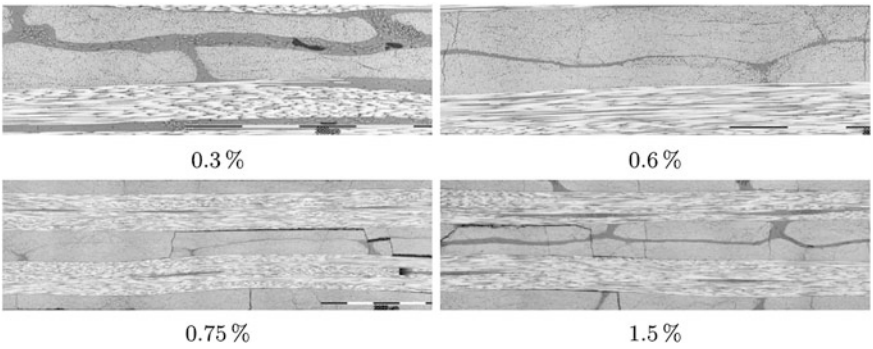

Fig. 12.2 Micrograph images at different strain levels

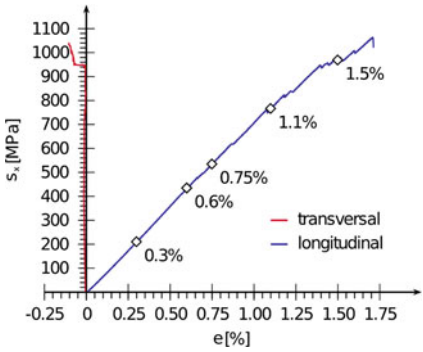

Fig. 12.3 Stress strain curve of NCF under quasi static load

At higher strain levels, these micro cracks starts to accumulate. At the strain level of 0.75%, first delamination damages are visible. In principle, half the ultimate strain level is sufficient to produce all damage phenomena, which finally results in the composite failure. At the strain level of 1.5% a high damage density can be observed.

It is important to understand that micro cracks often are delamination onsets and enable a delamination growth through the plies. Furthermore they can bridge delaminations across single plies. In general, it is not possible to test a single intralaminar failure mode separately.

The corresponding stress strain curve in Fig. 12.3 shows nearly linear material behaviour. The ultimate material strength is identified by the load drop-off.

12.3 Interlaminar Test Methods

The complex failure behaviour of composites motivated many authors to develop different interlaminar test methods. Several test concepts, specimen designs and test-setups exist, but only a few of them produce test results for combined through-thickness loading conditions and none of them with acceptable accuracy and reproducibility.

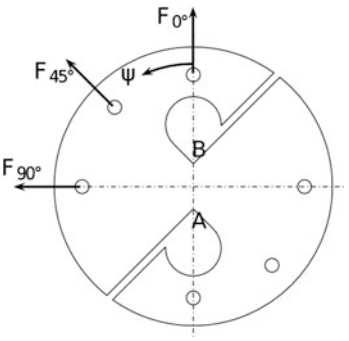

Fig. 12.4 Specimen geometry used by Arcan [6]

Some test methods determine appropriate single interlaminar properties. The Iosipescu test used by Adams et al. [1] determines representative interlaminar shear properties of composites. In principle, this test can also be used to test combined load conditions. Balakrishnan et al. [2] and Bansal et al. [3] determined combined interlaminar shear and compressive properties through a modified bi-axial Iosipescu test. The double notched and rail shear tests are further possibilities to determine interlaminar shear properties, but with these tests no combined load conditions can be applied. Furthermore, Uenal et al. [4] and Hussain et al. [5] noticed that bending stresses are superposed on the shear stress state, which causes inaccurate interlaminar properties. Another popular method is to bend flat or curved specimens. Avva et al. [6] and Greszczuk et al. [7] developed curved specimens and determined the interlaminar properties. In general, bending causes normal and shear stress components leading to relative complex stress states. The determination of one single strength property is often difficult or not possible.

A method to analyse combined tensile and shear loads was originally published by Arcan et al. [8]. Arcan has developed the specimen shown in Fig. 12.4 with two asymmetric cut-outs. The specimen can be installed at different angles into a uni-axial standard test device. Depending on the direction, single and combined shear or tensile stress states are generated within a defined cross section (points A and B). The sophisticated specimen geometry is a disadvantage, as it is generally difficult to produce.

El-Hajjar et al. [9] published a modified concept with a smaller specimen geometry, which is clamped to a steel fixture. Both test setups determine intralaminar in-plane material properties and focus on determining properties for shear loading.

12.4 A Test Setup for Interlaminar Properties Under Combined Loading

The concept acc. Fig. 12.5 has been developed to test combined and single interlaminar properties. The test device allows measurement of properties for single shear, tension and compression loads, as well as for combined shear loads.

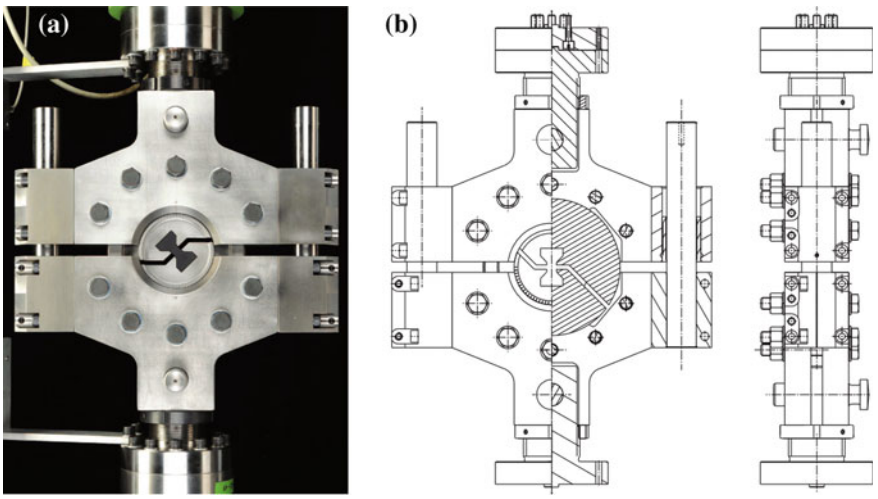

Fig. 12.5 Bi-axial test device to determine interlaminar properties

The concept differs from other Arcan test concepts by the pair of lubricated linear ball bearing systems on both sides of the test device. They provide a defined movement of the test rig and therewith a precise deformation of the specimen. Different types of specimen geometries can be tested by changing a rotatable insert inside the test rig. This insert can be used in different orientations between 0 and 90° angles. The specimen is tested without any clamping or adhesive bonding. This enables high test rates, but requires accurate production of specimen geometries.

12.4.1 Material Preparation and Specimen Production

The specimens are produced from a flat NCF plate with a moderate thickness of approximately 30 mm. The specimen plate used for the test is made of 60 NCF plies in a symmetrical layup. Each NCF ply consists of two orthogonal single unidirectional plies. The specimen plate is produced with the resin infusion technology through an autoclave process.

A representative test requires homogeneous stress distributions within the test sections of the specimens. It was found that tensile and shear loads cannot be tested with identical geometries. Therefore, two types of specimen geometries are designed. The tension specimen in Fig. 12.6 was primarily developed to determine interlaminar properties under tensile loads. The tensile specimen is manufactured with additional E-glass/epoxy composite tabs on the upper and the lower side of the specimen. FE simulations revealed that the best homogenous tensile stress distribution is generated with a specimen radius of 12 mm.

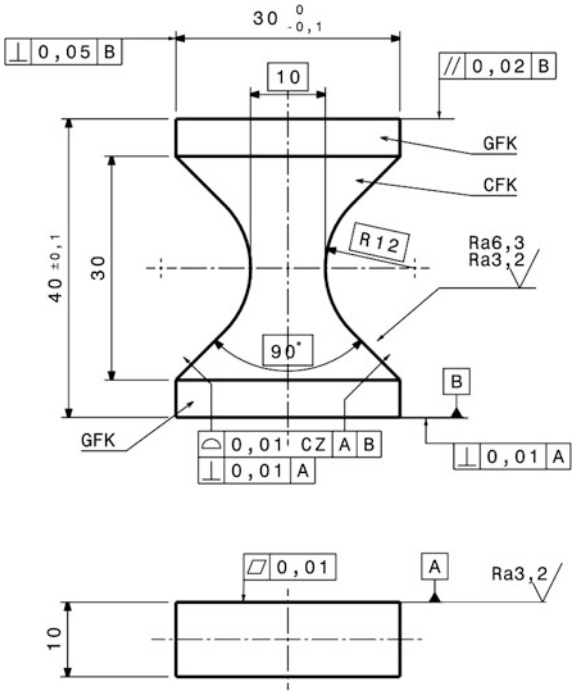

Fig. 12.6 Interlaminar tensile specimen

The specimen in Fig. 12.7 is used to determine interlaminar properties under shear loads as well as for combined loading. It was found that a notch radius of 1 mm provides the best compromise between a narrow notch to generate homogeneous shear stress distributions and a representative part of the cross-ply NCF for the shear specimen.

The tested cross section of both specimens has a width of 10 mm and a length of 10 mm. The specimens are tested without clamping or bonding. Therefore the test load introduction into the specimen is critical. The rectangular contour of the shear specimen provides a reliable load transfer. The load is introduced into the tension specimen via wedges on the upper and the lower side of the specimen.

12.4.2 Testing and Analysis of the Results

It is assumed that the applied test force F_p is always a superposition of a normal

$$F_{p,N} = F_p \cos \psi \tag{12.1}$$

and a transversal

$$F_{p,T} = F_p \sin \psi \tag{12.2}$$

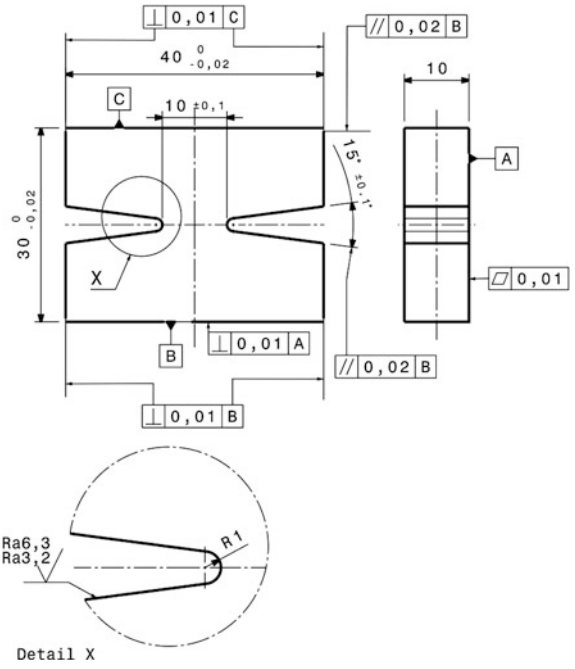

Fig. 12.7 Interlaminar shear specimen

component. It can therefore be split into two terms according to the orientation angle ψ of the specimen in relation to the machine coordinate system of the test device. The load ratio

$$f_{biax} = \frac{F_{p,N}}{F_{p,T}} \tag{12.3}$$

determines the ratio between longitudinal and transversal loading. Table 12.2 uses this load ratio to determine the failure load under combined loading.

Furthermore, it is assumed that the specimens will fail at their narrowest cross section. Accordingly, this section determines the material strength properties.

Figure 12.8 shows the stress strain curves of the interlaminar shear and interlaminar tensile tests. The results for the various similar test specimens show that the test determines consistent and reliable material properties.

The specimen failure and the maximum interlaminar strength are clearly identified by the load drop of the stress strain curve. The determination of the material strength under compression is more difficult, because the measured test result could not be conclusively assigned to the compression strength. Figure 12.9 shows two test results for combined compression-shear loads. The 45° loading angle corresponds to a balance of shear and compression. It shows a load drop at approximately 13 kN test force. At a load ratio corresponding to a 60° angle in the test device, i.e. leading to a slightly higher compression, no load drop is observed anymore. Although compressive loads cause micro-cracks, the material can be

Table 12.2 Interlaminar strength under combined and single loads

Specimen	Load ratio (%) f_{biax}	Tension/compression max. strength [MPa]	Shear max. strength [MPa]
Tension	0	41,123.83	0
Shear	0	0	47,725.51
Shear	15	−15,861.01	59,203.73
Shear	30	−42,464.39	73,544.39
Shear	45	−91,628.24	92,628.24
Shear	60	−137,6679.48	11,366.56

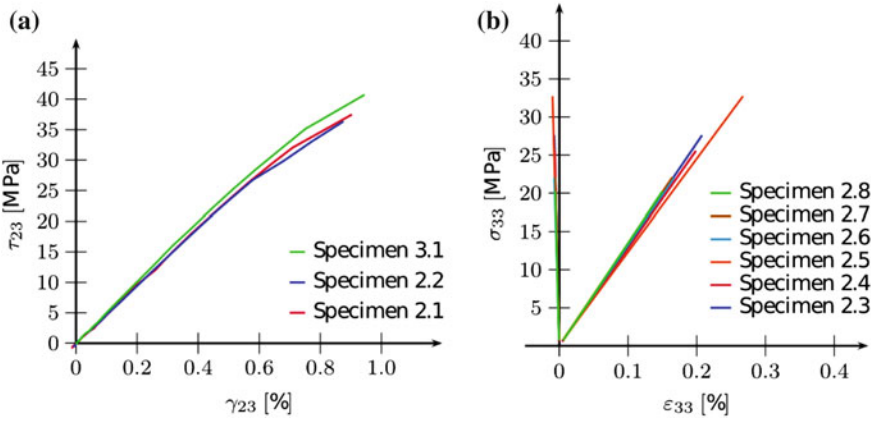

Fig. 12.8 Load–displacement curve for the shear and tensile test. **a** Interlaminar shear load. **b** Interlaminar tension load

continuously loaded. Under high compression load the specimen does not fail by separation, i.e. breaking into two parts, as observed under tensile or shear loads. Therefore, combined shear-compression properties at higher compression or pure compression strength properties could not be determined by the analysis of the load displacement curve. But combined shear-compression strength can be determined up to the limit of a balanced compression-shear load ratio corresponding to a 45° angle on the test device.

To determine compression strength at higher compression-shear load ratios, it is assumed that the strength can be specified at the first discontinuity of the load displacement curve.

12.4.3 Results for Combined Interlaminar Loads

Figure 12.10 shows test results for tensile as well as for combined shear and compression loads. It was found that the overall strength increases with a growing compression to shear ratio up to a certain limit. It was observed that the scatter of

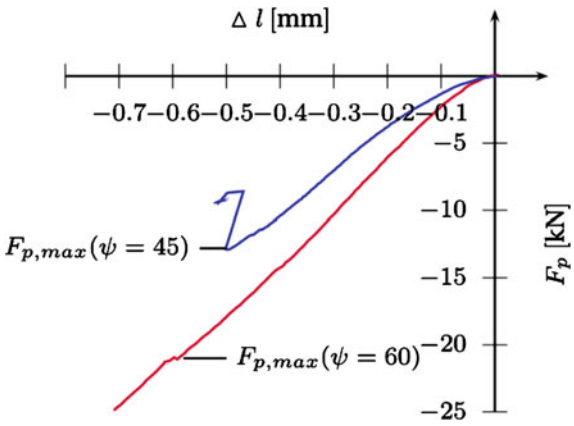

Fig. 12.9 Combined compression-shear load-displacement curve

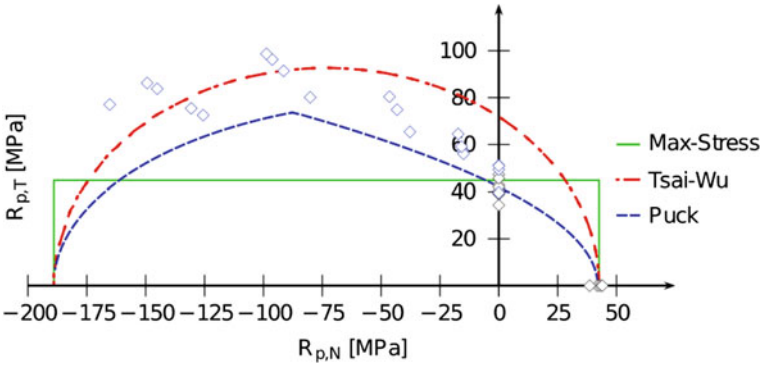

Fig. 12.10 Interlaminar material strength and failure criteria envelops

test results becomes larger for increasing load ratios. The interlaminar tensile strength is nearly equal to the intralaminar strength in Table 12.1. This is in good agreement with the assumption that a thick composite material provides the same intralaminar and interlaminar tensile strength transversal to the fiber direction.

The measured strength values are summarised in Table 12.2. The interlaminar tension strength has been determined with tension specimens, the combined interlaminar shear and compression strength with shear specimens. The biaxial load ratio f_{biax} defines a relation of the compression or tensile strength normal and transversal to the material orientation according to equation [6].

Figure 12.10 also shows the interlaminar strength prediction according to the maximum stress criterion, to the polynomial criterion of Tsai and Wu [10] and to the fracture hypothesis of Puck. According to Puck and Tsai-Wu the failure envelopes increase under combined shear and compression loads. The maximum stress criterion provides a rough approach with a constant behaviour under

combined interlaminar loads. Especially the hypothesis of Puck provides an adequate approximation of the failure envelope. Although the increase in strength under increasing compression-shear ratio is also predicted by Tsai and Wu, their criterion uses the intralaminar shear strength to also predict the interlaminar shear strength and overestimates the maximum strength under interlaminar shear loads.

It shall be noticed that all failure approaches are based on linear elastic material behaviour, whereas the measurements reveal a nonlinear material behaviour, even before the material strength limit is reached.

12.5 Conclusion

Research so far has been mainly focused to the composite failure mechanism due to intralaminar loading, whereas the interlaminar failure behaviour under combined loads in the thickness direction has been treated relatively seldom in the literature. Micrograph images of NCF laminates tested under in-plane loads show damages in different interacting inter-fiber modes. Micro cracks, which are an intralaminar failure mode, interact with interlaminar damage modes. A new test setup enables the determination of interlaminar properties under combined load conditions. The advantage of the presented test method is the determination of interlaminar strength properties of composite under well defined combined load cases. The test results show an increasing strength towards increasing compression-shear load ratios. This behaviour corresponds to the failure envelopes of the hypothesis from Puck and Tsai-Wu, but the onset of damage starts at lower load levels. Although the known failure hypothesis corresponds to the measurements, the nonlinear damaging behaviour is not covered.

References

1. Adams, D.F., Lewis, E.Q.: Experimental strain analysis of the Iosipescu shear test specimen. Exp. Mech. **6**, 352–360 (1995)
2. Balakrishnan, M.V., Bansal, B., Kumosa, M.: Biaxial testing of unidirectional carbon-epoxy composite using biaxial Iosipescu test fixture. J. Compos. Mater. **31**, 486–508 (1997)
3. Bansal, A., Kumosa, V.: Application of the biaxial Iosipescu method to mixed-mode fracture of unidirectional composites. Int. J. Fract. **71**, 131–150 (1995)
4. Ünal, O., Bansal, N.P.: In-plane and interlaminar shear strength of a unidirectional hi-nicalon fiber-reinforced celsian matrix composite. Nasa Technical Report NASA/TM 2000-210608, National Aeronautics and Space Administration, Glenn Research Center, NASA Center for Aerospace Information 7121 Standard Drive Hanover, MD 21076, Dezember 2000.
5. Hussain, A.K., Adams, D.F.: Analytical evaluation of the two-rail shear test method for composite materials. Compos. Sci. Tech. **64**(2), 221–238 (2004)
6. Avva, H.S., Allen, H.G., Shivakumar, K.N.: Through the thickness tension strength of 3-d braided composites. J. Compos. Mater. **30**(1), 51–69 (1996)

7. Hartung, D.: Materialverhalten von Faserverbundwerkstoffen unter dreidimensionalen Belastungen. DLR Forschungsbericht 2009–2012, Fakultät für Maschinenbau, Technische Universität Braunschweig (2009)
8. Arcan, M., Hashin, Z., Voloshin, A.: A method to produce uniform plane-stress states with applications to fibre-reinforced materials. Exp. Mech. **18**, 141–146 (1977)
9. Gning, P.B., Delsart, D., Mortier, J.M., Coutellier, D.: Through-thickness strength measurements using Aran's method. Compos. B **41**, 308–316 (2010)
10. Tsai, S.W.: Theory of composites design. ISBN 0-9618090-3-5. Think composites, think composites, Dayton, USA, 1 edn, 1992